EPJ Web of Conferences **75**, 09004 (2014)
DOI: 10.1051/epjconf/ 20147509004

XAFS studies of diluted magnetic semiconductor Mn-doped $ZnSnAs_2$ thin films on InP substrates

H. Oomae[1], H. Toyota[1], S. Emura[2], H. Asahi[2], and N. Uchitomi[1,a]

[1]Department of Electrical Engineering, Nagaoka University of Technology, Niigata, Japan :
[2]The Institute of Scientific and Industrial Research, Oosaka University, Oosaka, Japan

Abstract. Mn-doped $ZnSnAs_2$ ($ZnSnAs_2$:Mn) thin films with 5.0 and 6.5% Mn composition were epitaxially grown by molecular beam epitaxy on InP (001) substrates. These films had a Curie temperature of 334 K, corresponding to room-temperature ferromagnetism. The local structures around Mn atoms in $ZnSnAs_2$:Mn were studied by analysis of the X-ray absorption fine-structure spectra. It was found that the Mn atoms substitute into Zn or Sn cation sites, and the Mn–As bond length is 2.50 Å, which is slightly smaller than the value of 2.53 Å in a sphalerite (zinc-blende) $ZnSnAs_2$ bulk crystal. The Mn–As bond length in $ZnSnAs_2$:Mn is consistent with the value obtained from GaMnAs, and has a smaller value than that obtained from the zinc-blend MnAs thin films grown on a InP substrate.

1 Introduction

Over the last two decades, III-V based diluted magnetic semiconductors (DMSs), as well as recently developed ferromagnetic metals such as half-metallic materials, have attracted much attention for use in spintronic devices and as candidates for beyond-CMOS technology. In particular, GaMnAs has been extensively studied from experimental and theoretical points of view, because it is well lattice-matched with GaAs substrates and shows a relatively high Curie temperature of more than 100 K [1-4]. Therefore, it has been considered to be a promising candidate for producing semiconductor spintronic devices.

As the alternative ferromagnetic semiconductors, II-IV-V_2 chalcopyrite semiconductors such as $CdGeP_2$[5], $CdGeAs_2$[6] and $ZnSnAs_2$[7-8] have been shown to become ferromagnetic by Mn doping, and have Curie temperatures higher than 300 K. A bulk-type $ZnSnAs_2$ crystal doped with Mn has been experimentally shown to be ferromagnetic at a high Curie temperature [7]. The magnetic ion Mn, which occupies the cation IV site in host chalcopyrite or zinc-blende (sphalerite) structures, has a local spin and at the same time acts as an acceptor. Very recently, $ZnSnAs_2$:Mn thin films have been epitaxially grown on InP (001) without any secondary phases, and have shown room-temperature ferromagnetism [8-10]. Both experimentally and theoretically, $ZnSnAs_2$ is probably regarded as a "vertical GaAs" to some extent, consisting of two interposing zinc-blende lattices, while permitting a high degree of Mn incorporation because Mn^{2+} ions may easily substitute on the group II Zn sites. The $ZnSnAs_2$ thin films grown by molecular beam epitaxy (MBE) tend to show zinc-blende structure rather than chalcopyrite structure, which is analogous to the GaAs zinc-blende structure with Ga atoms being randomly replaced with either a Zn or Sn atom. Therefore, the ternary compound $ZnSnAs_2$ grown by MBE is referred to as zinc-blende $ZnSnAs_2$. On the basis of the present results, this material has the potential to produce InP-based spintronic devices, for which the lattice-matched III-V semiconductors InGaAs and InAlAs are expected to make possible magnetic quantum-well structures. However, the state of research and development of ferromagnetic II-IV-V_2 chalcopyrite semiconductors is still at the very early stage, and basic information is still not available on the parameters needed for spintronic device application.

X-ray absorption fine structure (XAFS) is a powerful tool for the study of the local structure around a specific component like Mn atoms in Mn-doped DMSs. This method offers important information on bond lengths and coordination numbers around the central atom, and helps us know which site the specific component occupies in the host material. Therefore, XAFS analysis has been effectively used for clarifying the physical properties of III-V based DMSs such as InMnAs [11], GaMnAs [12] and GaCrN [13]. In the case of the GaMnAs, it has been reported that the Mn atoms are substituted into the Ga sites and the Mn–As bond (0.249–0.250 nm) is slightly elongated from the Ga–As bond of the GaAs lattice. In contrast to the systematic investigation of III-V based DMS thin films, there have been few opportunities to study the structural properties of II-IV-V_2 based DMS thin films until now.

[a] Corresponding author: uchitomi@nagaokaut.ac.jp

In this paper, we report on the local structure around the Mn atoms in the $ZnSnAs_2$:Mn thin films grown epitaxially on InP substrates using Mn *K*-edge XAFS.

2 Experimental procedure

$ZnSnAs_2$ films doped with 5.0% and 6.5% Mn content were mainly employed for this experiment. The $ZnSnAs_2$:Mn films were grown on semi-insulating InP (001) substrates in a MBE chamber using solid elemental sources. Using the optimum substrate temperature of 300 °C and a Zn:Sn:As_4 beam equivalent pressure (BEP) ratio of 24:1:52, we grew a 100-nm-thick $ZnSnAs_2$ epitaxial film doped with 5.0% or 6.5% Mn on a 16-nm $ZnSnAs_2$ buffer layer. The detailed growth procedure of $ZnSnAs_2$:Mn films on InP (001) has been published [9-10]. High-resolution X-ray diffraction (HR-XRD) measurements were performed to determine the lattice constant of the samples. Superconducting quantum interference device (SQUID) magnetometry was used to investigate the magnetic properties of the $ZnSnAs_2$:Mn thin films.

X-ray absorption spectroscopic measurements of the XAFS spectra were performed at a beamline BL9A in PF, KEK. The beamline BL9A was installed with a Si (111) double-crystal monochromator and a pseudo-conical shape mirror for collimation of incident X-rays. The XAFS spectra at the Mn K-edge from $ZnSnAs_2$:Mn thin films were recorded in fluorescence mode in an almost total reflection configuration, using a solid-state detector (SSD, Ge:Li) with 19 elements. A high-purity (99.95%) aluminum pipe was set just before the sample to block the detector reception of elastic and inelastic scattering by air in the X-ray path to the sample. The incident X-ray energy was calibrated at the pre-edge of the Cu foil (12.7185 degrees). The typical sample size was 5 mm in width and 10 mm in length. All measurements were run at room temperature. The observed XAFS spectra were analyzed by the code REX2000.

3. Results and discussion

Figure 1 shows the high-resolution XRD profiles close to the InP (004) reflection observed for 5.0% and 6.5% Mn-doped $ZnSnAs_2$ thin films. As seen from the patterns, the reflection peaks from Mn-doped and buffer $ZnSnAs_2$ thin films, respectively, are clearly separated into 62.76° and 63.07°, suggesting that these samples were successfully prepared. The diffraction patterns showed no traces of the other phase or Mn precipitates. A diffraction peak from the $ZnSnAs_2$ buffer layer was also observed for the 5.0% Mn-doped $ZnSnAs_2$ thin film.

Figures 2(a) and (b) show the magnetization values *M* as a function of the magnetic field *H* for 5.0 and 6.5% Mn-doped $ZnSnAs_2$ thin films observed at 300 K, respectively. It should be mentioned that the *M-H* curves shown here were generated by subtracting the diamagnetic response of the underlying InP substrates. The hysteresis loops of both Mn-doped $ZnSnAs_2$ thin films were clearly observed even at 300 K. The *M-T* curves (not shown here) were measured from 5 to 400 K, and showed ferromagnetism with a Curie temperature of 334 K.

The XAFS oscillations $\chi(k)$ were extracted by the code REX2000 from the observed spectra, and weighted by k^3 in order to compensate for the damping of the XAFS amplitude with increasing *k*, where *k* is the wave-number of the excited electron in the free space. Figures 3 (a) and (b) show the XAFS oscillations weighted with k^3 for

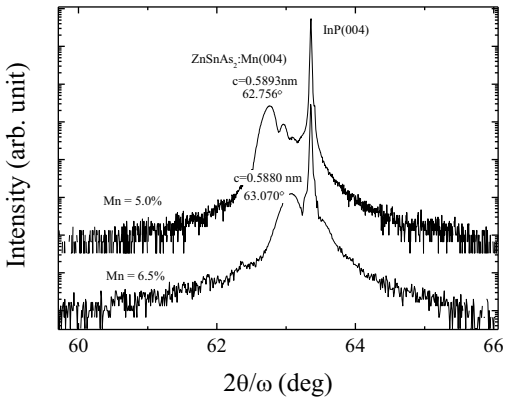

Figure 1. High-resolution XRD profiles of Mn-doped $ZnSnAs_2$ thin films with Mn concentations of 5.0 % and 6.5% on InP (001) substrates.

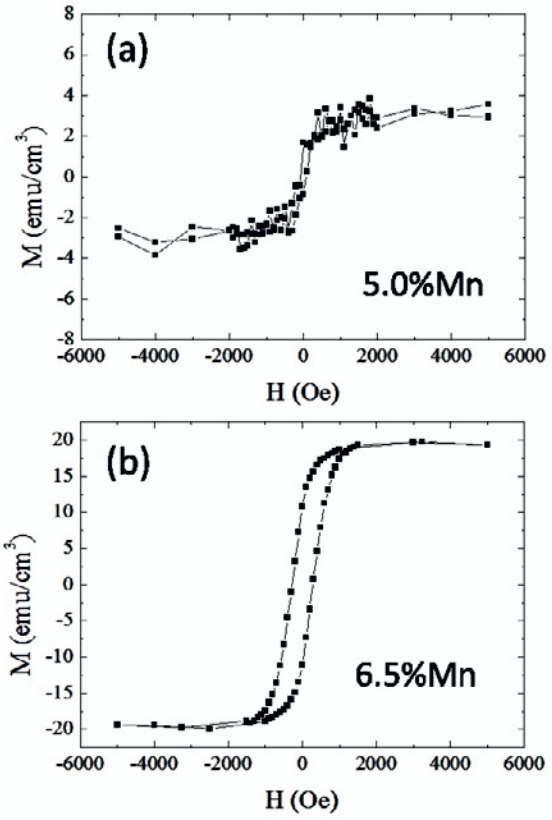

Figure 2. Magnetization as a function of applied field for (a) 5.0 % and (b) 6.5 % Mn-doped $ZnSnAs_2$ thin films at 300 K.

$ZnSnAs_2$ thin films doped with 5.0 and 6.5 % Mn, respectively. The $k^3\chi(k)$ oscillations were Fourier-transformed within k = 2 ~ 15 Å $^{-1}$ to obtain a radial distribution function (RDF) as shown in Figs. 4 (a) and (b). The RDF shows an apparent peak at around 2.2 Å, which corresponds to the scattering of photoelectrons due to the nearest neighbor atom, As. In contrast, although the smaller peaks from the second-nearest neighbor atoms are expected to appear at around 3.8–3.9 Å, they are not well defined. The curve-fitting process for the dominant peak at 2.2 Å was run to search the exact local structural quantities of the first-nearest neighbor. Figures 5 (a) and (b) show both spectra of the reverse Fourier transformation of the dominant first peak and the best-fitted oscillation. The agreement is excellent as indicated by the very low values of the reliability factor (R-factor) given in Table 1. Here, it is assumed that the nearest neighbor atom is As. From this result, the second-nearest neighbor atoms might vary in terms of the positions of Zn and Sn because of their disordering. This result was supported from local three-dimensional structure analysis of $ZnSnAs_2$:Mn thin films by X-ray fluorescence holography [14]. The local structural quantities around the Mn atom in the Mn-doped $ZnSnAs_2$ thin films obtained from the curve-fitting process are listed in Table 1. The average distance of four arsenic atoms surrounding the central Mn atom was determined to be 2.50 Å. The bond lengths of both Mn_{Zn}–As and Mn_{Sn}–As in these $ZnSnAs_2$:Mn films were found to be elongated, which might be ascribed to the large atomic radius of Mn compared with Zn.

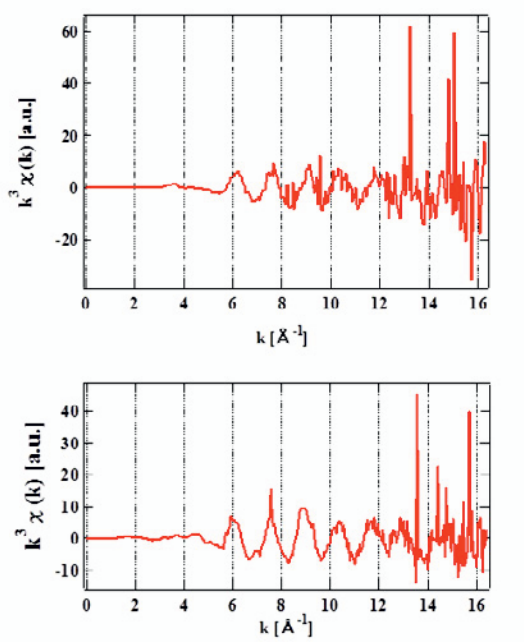

Figure 3. XAFS χ function weighted with photoelectron wave number k^3 for $ZnSnAs_2$ thin films doped with 5.0% and 6.5 % Mn.

The growth of zinc-blende (zb) type MnAs thin films on InP (001) substrates has been reported [15]. The zb-type MnAs thin films are pseudomorphically lattice-matched with InP (001) substrates. The free-standing lattice constant of zb-type MnAs was obtained as 6.068 Å or 6.060 Å by high-resolution X-ray diffraction. The Mn-As bond length was estimated to be 2.63 or 2.62 Å. The expected Mn–As bond length of the zb-type MnAs was reported to be 2.55 Å since the lattice constant of zb-MnAs predicted from the linear extrapolation of the experimental lattice constant of $Ga_{1-x}Mn_xAs$ for x → 1 was 5.89 Å [16]. The Mn–As bond length in the GaMnAs was measured by XAFS to be 2.49–2.50 Å, which is slightly compressed compared with the expected Mn–As

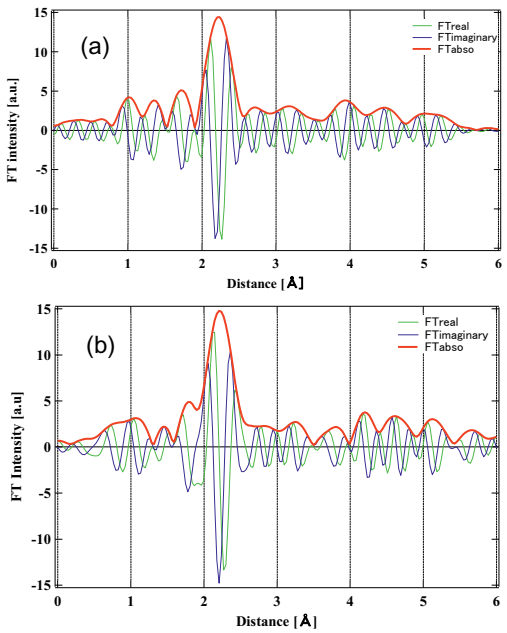

Figure 4. Fourier transform (radial distribution function) around the Mn atom in Mn-doped $ZnSnAs_2$ with Mn concentrations of (a) 5.0% and (b) 6.5%.

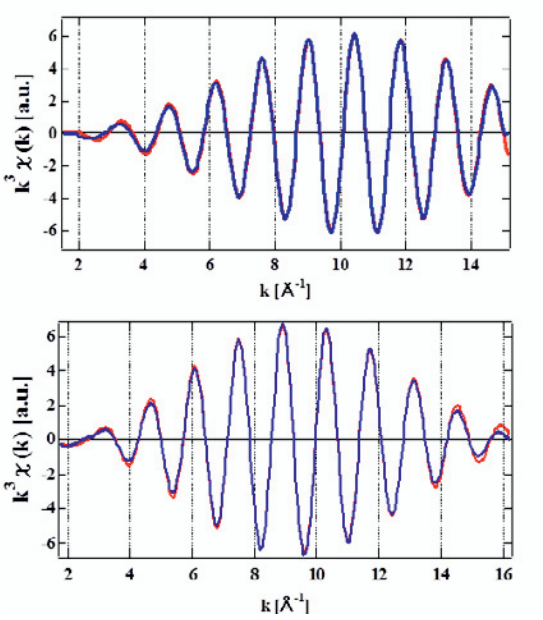

Figure 5. Simulated XAFS χ function weighted with photoelectron wave number k^3 for $ZnSnAs_2$ thin films doped with 5.0% and 6.5 % Mn.

bond length. The Mn–As bond length of zb-type MnAs grown on InP is larger than that of zb-type MnAs grown on GaAs, In contrast, the Mn–As bond length in $ZnSnAs_2$:Mn is well consistent with the value obtained from GaMnAs.

Table 1. Summary of curve fitting results

sample	*N*	R (Å)	R-factor (%)
5% Mn:$ZnSnAs_2$	3.9	2.50	0.19
6.5% Mn:$ZnSnAs_2$	4.7	2.51	0.25

4. Conclusion

$ZnSnAs_2$:Mn thin films with 5.0% and 6.5% Mn composition were epitaxially grown by molecular beam epitaxy on InP (001) substrates. These films had a Curie temperature of 334 K, corresponding to room-temperature ferromagnetism. The local structures around Mn atoms in the $ZnSnAs_2$:Mn were studied by XAFS measurements. It was found that the Mn atoms were substituted into Zn or Sn cation sites, and the Mn–As bond length was 2.50 Å, which is slightly smaller than the value of 2.53 Å in sphalerite (zinc-blende) $ZnSnAs_2$ bulk crystal.

Acknowledgement

X-ray spectra measurements at the Photon Factory (beamline BL9A) of KEK were performed in cooperation with the Institute of Material Structure Science under Proposal No. 2011G173.

References

1. H. Ohno, Science **281**, 951 (1998).
2. T. Jungwirth, J. Sinova, J. Masek, K. Kucera, A. H. MacDonald, Rev. Mod. Phys. **78**, 809 (2006).
3. T. Dietl, H. Oono, F. Matsukura, Phys. Rev. B **63**, 195205 (2001).
4. S. Sato, M. A. Osman, Y. Jinbo, N. Uchitomi, Appl. Surf. Sci. **242**, 134 (2005).
5. G. A. Medvedkin, T. Ishibashi, T. Nishi, K. Hayata, Y. Hasegawa, K. Sato, Jpn. J. Appl. Phys. **39**, L949 (2000).
6. R. Demin, L. Koroleva, S. Marenkin, S. Mikhailov, T. Aminov, H. Szymczak, R. Szymczak, M. Baran, J. Magn. Magn. Matter. **290-291**, 1379 (2005).
7. S. Choi, G. B. Cha, S. C. Hong, S. Cho, Y. Kim, J. B. Ketterson, Y. -Y. Jeong, G. C. Yi, Solid State Commun. **122**, 165 (2002).
8. J.T.Asubar, Y.Jinbo, N.Uchitomi, J. Cryst. Growth **311**, 929 (2009).
9. N. Uchitomi, H. Oomae, J. T. Asubar, H. Endo, Y. Jinbo, Jpn. J. Appl. Phys. **50**, 05FB02 (2011).
10. H. Oomae, J. T. Asubar, Y. Jinbo, N. Uchitomi, Jpn. J. Appl. Phys. **50**, 01BE12 (2011).
11. Y. L. Soo, S. W. Huang, Z. H. Ming, Y. H. Kao, H. Munekata, L. L. Chang, Phys. Rev. B **53**, 4905 (1996).
12. R. Shioda, K. Ando, T. Hayashi, M. Tanaka, Phys. Rev. B **58**, 1100 (1998).
13. M. Hashimoto, H. Tanaka, S. Emura, M. S. Kim, T. Honma, N. Umesaki, Y. K. Zhou, S. Hasegawa, H. Asahi, J. Cryst. Growth **273**, 149 (2004).
14. K. Hayashi, N. Uchitomi, J. T. Asubar, N. Happo, W. Hu, S. Hosokawa, M. Suzuki, Jpn. J. Appl. Phys. **50**, 01BF05 (2011).
15. H. Oomae, J. T. Asubar, S. Nakamura, Y. Jinbo, N. Uchitomi, J. Cryst. Growth **338**, 129 (2012).
16. M. Shirai, T. Ogawa, I. Kitagawa, Suzuki, J. Magn. Magn. Matter. **177**, 1383 (1998).